

The role of solar-like magnetic activity in the evolution of single stars, binaries and star-planet systems

Scientific report

This report is a summary of our most important scientific results achieved in the framework of our OTKA/NKFI research contract K-109276. Most of the following results have already been published in high-impact journals.

Preamble

In the past decade studying the origin of solar and stellar magnetic activity and the impact of magnetism on the cosmic environment has become a current intriguing issue. This is, because the Sun and Sun-like dwarf stars are supposed to provide relatively stable cosmic environment for billions of years, offering favourable conditions for life to grow up on the surface of orbiting rocky planets. However, in certain circumstances, stellar activity itself can be one of the main threats to habitability as well. Therefore, in order to understand the role of magnetic activity in the evolution of stars and their environment, it is essential to set up a general view of magnetic activity. This can be characterized by revealing the similarities and differences between the directly observable active Sun in the nearby and the more distant active stars, which are mostly unresolved bright points in the sky, but countless. In our research program we have focused on observing the components of the magnetic dynamo, i.e., the mechanism responsible for reproducing and magnifying the stellar magnetic fields on different spatial and temporal scales. Dynamo mechanism can be influenced by tidal interactions in star-star and even star-planet systems as well. Therefore, to study the role of such a tidal feedback, we have compared the working dynamo characteristics in single stars to components of close binary systems. The most important results are summarized as follows.

New scientific results achieved during the project

1 Solar magnetic fields and solar activity

1.1 The role of evolving active regions in redistributing solar magnetic fields

Solar active regions (AR) are centres of magnetic activity. As new flux emerges into a pre-existing magnetic environment, its evolution leads to re-configuration of small- and large-scale magnetic connectivities. The decay process of ARs spreads the once-concentrated magnetic flux over an ever-increasing area. Though most of the flux disappears through small-scale cancellation processes, it is the remnant of large-scale AR fields that is able to reverse the polarity of the poles and build up new polar fields. Since large-scale flux is generated by the deep-seated solar dynamo, the observed characteristics of flux emergence and that of the subsequent decay provide vital clues as well as boundary conditions for dynamo models.

We presented a contemporary view of how solar active region magnetic fields are understood to be generated, transported and dispersed. Empirical trends of active region properties that guide model development are discussed. Physical principles considered important for active region evolution are introduced and advances in modeling are reviewed. We reviewed solar indices, always emphasizing the physics they represent, which were developed and are being widely used to monitor the level of solar activity and study the solar cycle. We reviewed evidence for twist/helicity in solar magnetic fields and made the link to the observed tilt angle of bipolar active regions, which plays important role in the solar cycle.

We explored the changes in coronal non-thermal velocity (V_{NT}) measurements at the solar poles from solar minimum to solar maximum of Solar Cycle 24. We found that there are no significant changes in the V_{NT} values over the cycle. The magnetic structures that create the enhanced V_{NT} behaviour were small-scale features and hence not easily measurable at the poles. Because they do not change during the solar cycle, they are likely to be created by a local dynamo.

We analyzed the evolution of the photospheric magnetic and velocity fields of the active region 10978 (AR), modelled its coronal magnetic field, and computed the location of magnetic null-points and quasi-separatrix layers (QSLs) searching for the origin of plasma upflows. We found that magnetic reconnection at the computed null points could not explain all of the upflow regions. However, upflows and QSLs were found to evolve in parallel, both temporarily and spatially. Our findings provide strong support to the results from previous individual case studies. We used local and global magnetic field modeling of the decaying active region to determine how the age of the active region impacts the extent of the open magnetic fields, and then how some of the upflows could become outflows. We found that the upflow speed and volume increase during the decay phase and that the plasma upflows become part of the solar wind through reconnection with magnetic field lines open towards the interplanetary space.

We studied how the magnetic field of a series of solar active regions (ARs) evolved with time to better characterise the emergence and dissipation of ARs. We examined the temporal variation in the magnetic field distribution of 37 emerging ARs. The results suggested that simple classical diffusion was not responsible for the observed changes in field distribution, but that other processes played a significant role in flux dispersion. We proposed that the steep negative slope seen during the late decay phase was due to magnetic flux reprocessing by (super)granular convective cells. We found as well, that convection might play an important role during the decay phase and also during the formation of active regions, particularly for low flux density values.

1.2 Formation and evolution of coronal mass ejections (CMEs)

Coronal mass ejections (CMEs) are one of the primary manifestations of solar activity and can drive severe space weather events. Therefore, it is vital to work towards being able to predict their occurrence. However, many aspects of CME formation and eruption are yet unclear.

We analysed the rotation of global EUV waves driven by CMEs in the solar lower corona. As suspected before, global EUV waves rotated in the same sense as the helicity in the CME source region. We analysed further 6 cases and found significant rotation in cases when the source region had a simple bipolar structure, and the rotation was indeed in the same sense as helicity in the source region. However, no rotation was observed when the CME-source active region had a complex magnetic structure. We interpreted the results based on differences in the interaction between the erupting magnetic flux rope and external simple or complex active region fields.

During the spectacular filament eruption (CME) on the 7th of June 2011, SDO/AIA images showed the appearance of brightenings at the place where the laterally expanding CME met with and compressed magnetic fields of a neighbouring active region. Through MHD simulations and analysis of the magnetic field topology at the location of the brightening we have provided evidence that the magnetic fields of the CME have reconnected with magnetic fields of the neighbouring active region and that the transient brightening resulted from in-situ plasma heating around the reconnection region.

We studied the pre-eruptive coronal configuration of an active region that produced an interplanetary CME with a clear magnetic flux rope structure at 1 AU. Extreme ultra-violet (EUV) coronal loops form a forward-S sigmoid two hours before the onset of the eruption (2012-06-14), which is interpreted as a signature of a right-handed flux rope that formed prior to the eruption. Flare ribbons and EUV coronal dimming regions are used to infer the locations of the flux rope footpoints. These locations, together with observations of the global magnetic flux distribution, indicate that an interaction between newly emerged magnetic flux and pre-existing sunspot field in the days prior to the eruption may have enabled the coronal flux rope to form via tether-cutting-like reconnection. Composition analysis suggests that the flux rope had a coronal plasma composition, supporting our interpretation that the flux rope formed via magnetic reconnection in the corona. Once formed, the flux rope remained stable for two hours before erupting as a CME.

We studied the variation of the accumulated coronal helicity derived from the magnetic helicity flux through the photosphere in active region (AR) NOAA 10365, where several large flares and coronal mass ejections (CMEs) occurred. We used SOHO/MDI full-disk line-of-sight magnetograms to measure the helicity flux, and the integral of GOES X-ray flux as a proxy of the coronal energy variations due to flares or CMEs. Using the linear force-free field model, we transformed the accumulated helicity flux into a time sequence of the force-free parameter α accounting for flares or CMEs via the proxy derived from GOES observations. This method can be used to derive the value of α at different times during the AR evolution, and is a partial alternative to the commonly used match of field lines with EUV loops.

1.3 Solar cycle correlation of coronal element abundances in Sun-as-a-star observations

The elemental composition in the coronae of low-activity solar-like stars appears to be related to fundamental stellar properties such as rotation, surface gravity, and spectral type. We used full-Sun observations from the Solar Dynamics Observatory EVE instrument to show that when the Sun is observed as a star, the variation of coronal composition is highly correlated with a proxy for solar activity, the F10.7 cm radio flux, and therefore with the solar cycle phase (see Figure 1). Similar cyclic variations should therefore be detectable spectroscopically in X-ray observations of solar analogs. The plasma composition in full-disk observations of the Sun is related to the evolution of coronal magnetic field activity. Our observations therefore introduce an uncertainty into the nature of any relationship between coronal composition and fixed stellar properties. The results highlight the importance of systematic full-cycle observations for understanding the elemental composition of solar-like stellar coronae.

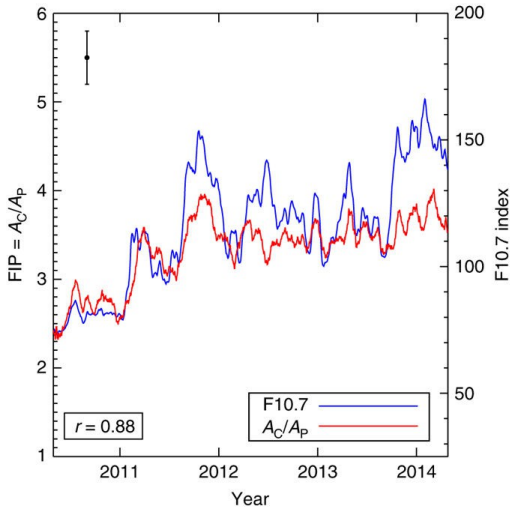


Figure 1. Correlation between the coronal to photospheric composition ratio and the F10.7 cm radio flux. The plot is taken from our paper by Brooks et al., *Nature Communications* 8, 183 (2017)

2 Stellar magnetic activity and the evolution of single stars, binaries and star-planet systems

2.1 Studying individual targets

We studied three overactive spotted K giants (IL Hya, XX Tri, and DM UMa) known to exhibit V-band light variations between 0.65-1.05 mag. Our aim was to find the origin of their large brightness variation. We emphasized that for IL Hya it was just about half of the total luminosity variation that could be explained by the photospheric temperature (spots/faculae) changes, while for XX Tri it was even about one third. The long-term, 0.6 mag V-band variation of DM UMa was more difficult to explain because little or no $B-V$ color index change was observed on the same timescale. Placing the three stars with their light and color variations into Hertzsprung–Russell diagrams, we found that their overall luminosities were generally too low compared to predictions from current evolutionary tracks. A change in the stellar radius due to strong and variable magnetic fields during activity cycles likely played a role in explaining the anomalous brightness and luminosity of our three targets. At least for IL Hya, a radius change of about 9% was suggested from bolometric magnitude and effective temperature, and was supported by independent $v \sin i$ measurements.

The active K1-giant component of the long-period RS CVn-type binary system σ Gem and its global surface flow pattern was revisited. We refined the differential rotation law from recovering the spot migration pattern. We applied a detailed cross-correlation technique to a unique set of 34 time-series Doppler images recovered using data from 1996/97. In addition, we presented a new time-series Doppler imaging study using our advanced surface reconstruction code *iMap* for a dataset collected in 2006/07. Results from the reprocessed cross-correlation study confirmed that the star was performing antisolar-type differential rotation with a surface shear of $\alpha = 0.04 \pm 0.01$, i.e., almost a factor of two stronger compared to the previously claimed value. We also confirmed the evidence of a global poleward spot migration with an average velocity of 0.21 ± 0.03 km/s, in accordance with theoretical predictions. From the new observations we obtained three subsequent Doppler images. The time evolution of these images confirmed the antisolar-type differential rotation of the same amount.

We investigated the surface spot activity of the rapidly rotating, lithium-rich active single K-giant DI Psc to measure the surface differential rotation and understand the mechanisms behind the Li-enrichment. Doppler imaging was applied to recover the surface temperature distribution in two subsequent rotational cycles. Surface differential rotation was derived by cross-correlation of the subsequent maps. Doppler images obtained for the Ca and Fe mapping lines agree well and revealed strong polar spottedness, as well as cool features at lower latitudes. We found antisolar differential rotation with shear coefficient $\alpha = -0.083 \pm 0.021$. We suggested that the lithium abundance was non-activity related.

We studied the connection between the chromospheric and photospheric behaviour of the active late-type star FK Comae. From low-resolution H α spectra we found that the changes in the chromosphere seemed to happen mainly on a time scale longer than a few hours, but shorter variations were also observed. Moreover, prominences were often found in the chromosphere that reached to more than a stellar radius and were stable for weeks, often connected to dark photospheric spots. The rotational modulation of the H α emission was typically anticorrelated with the light curve, but we did not find convincing evidence of a clear connection in the long-term trends of the H α emission and the brightness of the star. In addition, FK Com seemed to be in an unusually quiet state in 2009-2010 with very little chromospheric activity and low spot contrast, which might indicate the long-term decrease in activity.

The spotted surface of the rapidly rotating but single K-giant KU Pegasi was investigated in order to detect its time evolution and to quantify the surface differential rotation. We presented 11 Doppler images from spectroscopic data collected between 2006-2011. The surface of KU Peg showed cool spots at all latitudes and one persistent warm spot at high latitude. A small cool polar spot existed for most but not all of the epochs. Differential rotation was extracted from these images by detecting systematic (latitude-dependent) spot displacements. We applied a cross-correlation technique to find the best fitting differential rotation law. Our analysis revealed solar-like differential rotation with a surface shear of $\alpha = 0.040 \pm 0.006$, i.e., approximately five times weaker than on the Sun. We also derived a more accurate and consistent set of stellar parameters for KU Peg including a small Li abundance of ten times less than solar and also concluded that the relatively rapid rotation of the star might be explained by one (or more) planet engulfment episode(s) at the beginning of the post-main sequence evolution.

The single rapidly rotating K-giant V1192 Ori was revisited to determine its surface differential rotation, lithium abundance, and basic stellar properties such as a precise rotation period. Stars with about 1-2 solar masses at the red giant branch (RGB), such like our target, represent an intriguing period of stellar evolution, i.e. when the convective envelope interacts with the fast-rotating core. During these mixing episodes freshly synthesized lithium can come up to the stellar surface along with high angular momentum material, altering the surface rotation pattern. Our aim was to independently verify the antisolar differential rotation of the star and possibly find a connection to the surface lithium abundance. We used our inversion code *iMap* to reconstruct 11 Doppler images from spectroscopic data collected with the STELLA robotic telescope between 2007-2016. We extracted the differential rotation from these images by tracing systematic spot migration as a function of stellar latitude from consecutive image cross-correlations. The position of V1192 Ori in the Hertzsprung-Russell diagram suggested that the star was in the helium core-burning phase just leaving the RGB bump. We measured $A(\text{Li})_{\text{NLTE}} = 1.27$, i.e. a value close to the anticipated transition value of 1.5 from Li-normal to Li-rich giants. Doppler images revealed extended dark areas arranged quasi-evenly along an equatorial belt. No cool polar spot was found during the investigated epoch. Spot displacements clearly suggested antisolar surface differential rotation with $\alpha = -0.11 \pm 0.02$ shear coefficient. We concluded that the surface Li enrichment and the peculiar surface rotation pattern might have indicated a common origin.

Stars that are more active than the Sun have more and stronger dark spots than does the Sun, including on the rotational pole. Doppler imaging, which has so far produced the most detailed images of surface structures on other stars, cannot always distinguish the hemisphere in which the starspots are located. This leads to problems in investigating the north-south distribution of starspot active latitudes; this distribution is a crucial constraint of dynamo theory. Indeed, polar spots, whose existence is inferred from Doppler tomography, could plausibly be observational artefacts. We reported imaging of the magnetically active giant star ζ Andromedae using long-baseline infrared interferometry for the first time. We confirmed the existence of a dark polar spot in each of two observation epochs. Lower-latitude spot structures in both hemispheres did not persist between observations, revealing global starspot asymmetries. The north-south symmetry of active latitudes observed on the Sun was absent on ζ And, which hosted global spot patterns that could not be produced by solar-type dynamos. The PI of our group was among the major contributors for this pioneering new research (see Figure 2).

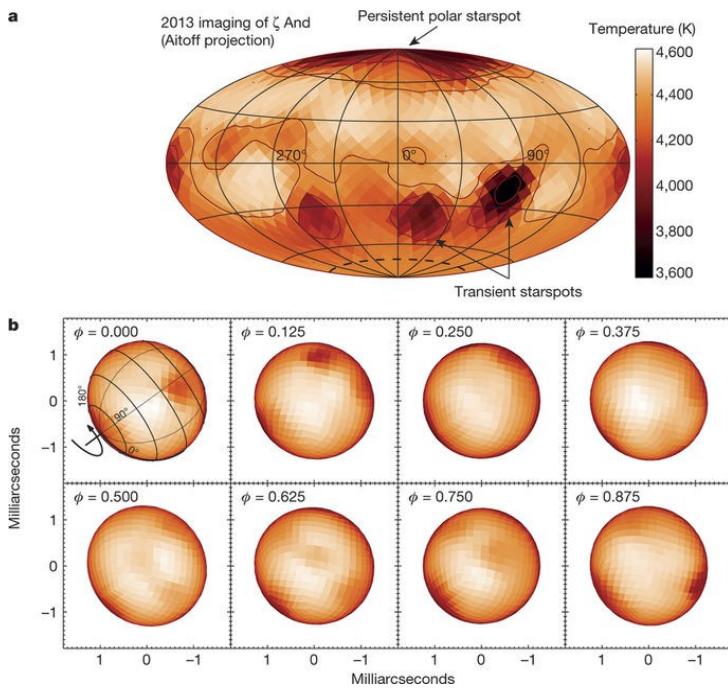


Figure 2. The first close-up pictures from the surface of a nearby star other than the Sun; see our paper by Roettenbacher et al., *Nature* 533, 217–220 (2016).

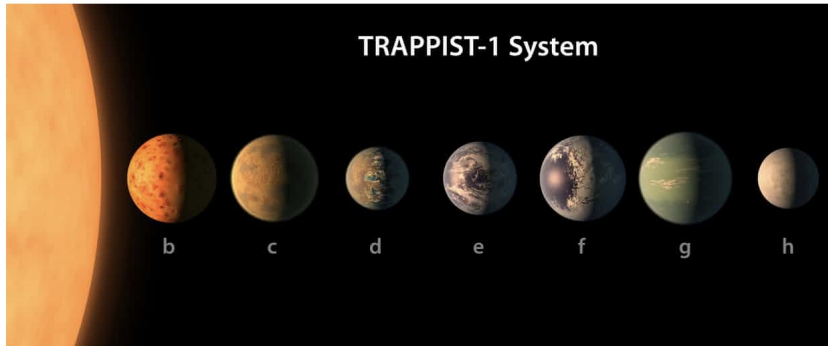
The ultrafast-rotating ($P_{\text{rot}}=0.44$ d) fully convective single M4 dwarf V374 Peg is a well-known laboratory for studying intense stellar activity in a stable magnetic topology. We analysed spectroscopic observations, $BV(RI)_C$ photometry covering 5 years, and additional R_C photometry that expands the temporal base over 16 yrs. The light curve suggested an almost rigid-body rotation and a spot configuration that was stable over about 16 yrs, confirming the previous indications of a very stable magnetic field. We observed small changes on a nightly timescale and frequent flaring, including a possible sympathetic flare. The strongest flares seemed to be more concentrated around the phase where the light curve indicated a smaller active region. Spectral data suggested a complex CME with falling-back and re-ejected material with a maximal projected velocity of ~ 675 km/s. We observed a CME rate that was much lower than expected from extrapolations of the solar flare-CME relation to active stars.

Over the duration of the Kepler mission, KIC 8462852 (also known as Tabby's star in the media) was observed to undergo irregularly shaped, aperiodic dips in flux of up to 20 per cent. The dipping activity can last for between 5 and 80 d. We characterized the object with high-resolution spectroscopy, spectral energy distribution fitting, radial velocity measurements, high-resolution imaging, and Fourier-analyses of the Kepler light curve. KIC 8462852 was found to be a typical main-sequence F3 V star with no significant IR excess, and without any (very close) interacting companion. We described various scenarios to explain the dipping events observed in the Kepler light curve. We concluded that the scenario most consistent with the data in hand was the passage of a family of exocomet or planetesimal fragments, all of which are associated with a single previous break-up event, possibly caused by tidal disruption or thermal processing. The minimum total mass associated with these fragments corresponds to an original rocky body of >100 km in diameter. The problem discussed in this paper needed the contribution of researchers from many different fields both in observational and theoretical works. Two members of our group are found among the major contributors.

We used high precision data from the Kepler mission to study the effect of stellar flares and coronal mass ejections on the exoplanetary system TRAPPIST-1, consisting of seven Earth-like exoplanets around an ultracool dwarf star. Our conclusion suggested that the magnetic activity of TRAPPIST-1 continuously altered the atmospheres of the orbiting exoplanets, probably making the planetary environment less favourable for hosting alien life. With this result we have accomplished a significant contribution to understanding how extraterrestrial life might be affected by the cosmic environment. Also, the resulting paper received extensive coverage on the media worldwide (see Figure 3).

The storm-lashed worlds of Trappist-1

The seven planets in orbit round a red dwarf star 39 light years away will provide valuable data about exoplanets and their atmospheres, but the latest data suggests that they are unlikely to be homely



▲ Artist's impression of Trappist-1's seven Earth-class planets. Photograph: NASA/PA

Figure 3. Lead paragraph of the article from *The Guardian* in 9 April 2017 reporting on our result claiming that the Trappist-1 system might be unsuited for alien life; see *Vida et al., The Astrophysical Journal 841, 124 (2017)*.

2.2 Surveys and statistical studies

We analysed light curves covering four years of 39 fast-rotating ($P_{\text{rot}} < 1$ d) late-type active stars from the Kepler data base. Using time-frequency analysis (short-term Fourier transform), we found hints for activity cycles of 300-900 d at 9 targets from the changing typical latitude of the starspots, which with the differential rotation of the stellar surface changed the observed rotation period over the activity cycle. We also gave a lowest estimation for the shear parameter of the differential rotation, which was around 0.001 for the cycling targets. These results populated the less studied, short-period end of the rotation-cycle length relation.

We searched the Kepler light curves of ~ 3900 M-star targets for evidence of periodicities that indicate, by means of the effects of starspots, rapid stellar rotation. We found 178 Kepler M-star targets with rotation periods, P_{rot} of < 2 days, and 110 with $P_{\text{rot}} < 1$ day. Some 30 of the 178 systems exhibited two or more independent short periods within the same Kepler photometric aperture, while several had 3 or more short periods. We concluded that the targets with multiple periods were very likely members of relatively young physical binary, triple, and even quadruple M-star systems. The $\sim 5\%$ occurrence rate of rapid rotation was consistent with spin evolution models that included an initial contraction phase followed by magnetic braking, wherein a typical M-star can spend several hundred Myr before spinning down to periods longer than 2 days.

From an examination of about 18,000 Kepler light curves of K- and M-stars we found some 500 which exhibited rotational periods of less than 2 days. Among such stars, approximately 50 showed two or more incommensurate periodicities. We found that these multiple periodicities are independent of each other and likely belonged to different, but physically bound, stars. Our result is potentially important for discovering young multiple stellar systems among rapidly rotating K- and M-dwarfs.

Recent space missions revealed that a high percentage of stars labeled as Cepheid candidates based on sparse photometric survey data were misclassified. We presented an analysis of three stars that had previously been identified, erroneously, as potential Cepheid variables. The stars were observed by the Kepler space telescope in Campaigns 0 and 2 of the K2 mission, and we concluded that their light variations were caused by stellar activity.

Using ESO facilities and the Nordic Optical Telescope we have obtained time series of multi-object spectroscopic observations of late-type stars in six open clusters with ages ranging from 15 Myrs to 300 Myrs. Additionally, we studied archival data of numerous active stars. These observations allowed us to obtain information on the occurrence rate of coronal mass ejections (CMEs) in late-type stars with different ages and spectral types.

We studied the different patterns of interannual magnetic variability in stars on or near the lower main sequence (solar-type G-K dwarf) stars in full time series of 36 yrs from the Mount Wilson Ca II *H&K* survey. We found at least one activity cycle on 28 of the 29 stars we studied. The stars formed two distinct groups: 12 stars, with longer and fairly similar rotational periods (39.7 ± 6.0 days) had simple smooth cycles with quite uniform lengths of 9.7 ± 1.9 yrs. The remaining 16 stars with much faster rotation (18.1 ± 12.2 days) had complex, sometimes vigorously changing multiple cycles on average of 7.6 ± 4.9 yrs. We found a clear age division between stars with smooth and complex cycles. The separation between the older and younger stars at around 2 to 3 Gyr of age, known as the Vaughan-Preston gap, follows from the rotational braking of the stars and the corresponding change in the stellar dynamo which drives the activity. The mean cycle period of the older group, where the Sun also belongs to, is about 10 yrs, very close to the sunspot cycle of 11 yrs. See Figure 4.

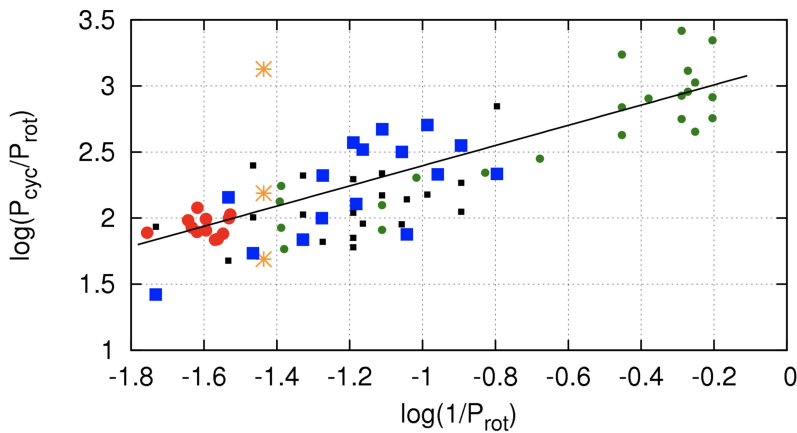


Figure 4. Relation between the observed rotational and cycle periods. The plot was taken from our paper by Oláh et al., *Astronomy & Astrophysics* **590**, A133 (2016)

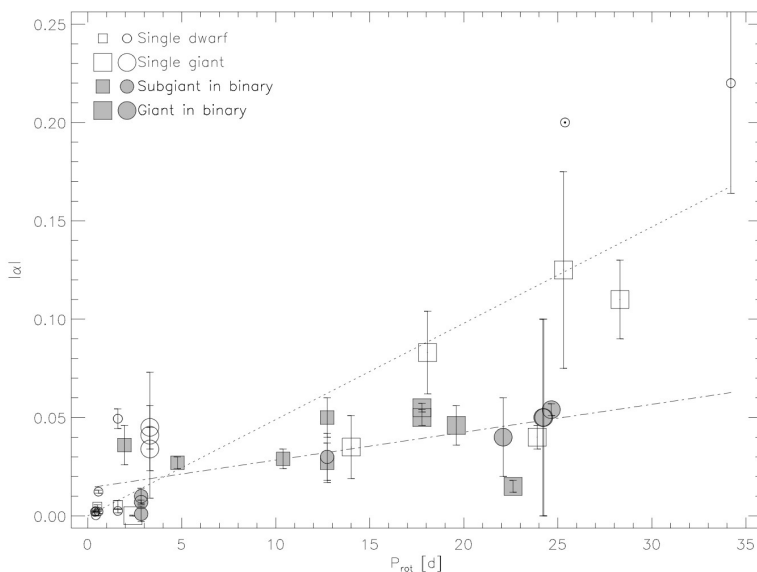


Figure 5. Rotation–differential rotation relationships for late-type stars. Plotted are the absolute values of the dimensionless surface shear parameter α vs. rotation period; see Kóvári et al., *Astronomical Notes* **338**, pp. 903-909 (2017).

Stellar dynamos are responsible for generating strong magnetic fields, however, dynamos work diversely in different types of stars, sometimes being at very different evolutionary stages. In our statistical analysis, from a suitable sample of spotted late-type stars showing surface differential rotation we found that the relationship between the rotation period and the surface shear coefficient α is significantly different for single stars compared to members in close binaries. Single stars followed a general trend that α increases with the rotation period. However, differential rotation of stars in close binary systems showed much weaker dependence on the rotation, if any, suggesting that in such systems tidal forces operated as a controlling mechanism of differential rotation. This result can be regarded as the most important synthesis of our work on observing stellar dynamos (see Figure5).

2.3 Reviews

We reviewed the most important observables that helped us to investigate stellar dynamos and compare those to the modelling results. We gave an overview of the available observational methods and data processing techniques suitable for such purposes, with touching upon examples of inadequate interpretations as well. Stellar observations were compared to the solar data in such a way, which ensured that the measurements were comparable in dimension, wavelength, and timescale.

We reviewed the current knowledge and status of investigations on the variable magnetic activity of cool stars. We discussed the Sun in the context of solar-type stars, highlighting peculiarities and common features in terms of its magnetic activity and variability over different time scales. We examined how both theory and observations were providing new clues about the main physical processes that generate magnetic fields in the interior of cool stars, as well as about those that led to evolving stellar surface magnetism and varying chromospheric and coronal phenomena. We discussed the relations between stellar age, rotation, and activity throughout the evolution of cool stars. We touched upon the importance of understanding stellar magnetism also in view of its effect on planetary environments.

3 Technical studies and developments to support astronomical data acquisition

Fly's Eye Camera System Project was funded within the Lendület-2012 grant by András Pál, one of the participants of our research team. This instrument was designed to obtain photometric data from the whole sky higher than 30 degrees above horizon by monitoring targets that are brighter than ~ 15 magnitude, i.e. suitable for monitoring of active stars as well. During the 4 years of our research program we were operating as a scientific support group for the technical development in the hopes of future monitoring of active stars by the Fly's Eye Camera System.

In the framework of our cooperation first we described a hexapod-based telescope mount system intended to provide sidereal tracking for the Fly's Eye Camera project. By exploiting such a meter-sized telescope mount, we built a device which was both capable of compensating for the apparent rotation of the celestial sphere enabling that the same design can be used independently from the actual geographical location. Our construction was demonstrated to have a sub-arcsecond tracking precision.

We described an alternative approach for generating pointing models for telescopes equipped with serial kinematics, esp. equatorial or alt-az mounts. Our model construction did not exploit any assumption for the underlying physical constraints of the mount. An advantage of our procedure was the fact that recovering the pointing model parameters, classical linear least squares fitting procedures could be applied. This parametrization also lacked any kind of parametric singularity, therefore it worked perfectly around the celestial poles. We demonstrated the efficiency of this type of model on real measurements related to the 1-meter RCC telescope operating at Pizskéstető. Here the absolute pointing results provided a root mean square accuracy of 1.5-2 arcseconds.

In order to attain precise, accurate and stateless positioning of telescope mounts we applied microelectromechanical accelerometer systems (also known as MEMS accelerometers). We investigated the advantages and challenges of applying such devices and to reach the sub-arcminute range. We presented how this accuracy could be achieved with very cheap MEMS sensors. We also demonstrated how our implementation can be inserted in a telescope control system.

Autonomous observations were performed by the Fly's Eye Camera system at Pizskéstető whenever weather permitted. We detailed the specifications of the camera-filter-lens optical setup and the custom solutions for fault-tolerant embedded control of the imaging subsystem. We demonstrated that even with this small-scale optics the accurate sidereal tracking was sufficient to reach millimagnitude precision at the bright-end while the detection of faint sources down to $r=15$ mag was also feasible with 2.5 min cadence. In addition, by summing up frames taken during a one-hour long series, it is also possible to go down even to $r \sim 17$ mag on the not-so-confused areas of the sky. The main goal of our project was to provide data series in the standard Sloan filters of continuously monitored various astronomical phenomena, including variability of stars with magnetic activity and transiting exoplanets.

4 Publication activity in numbers

Altogether **43 publications** were listed in the closing report; **38** were published as **refereed papers**, mostly in high-impact journals. Among them, one paper appeared in *Nature*, one in *Nature Communications*, and four review papers were published in *Space Science Reviews*. Our publication activity yielded a **cumulative impact factor** of **231.415**.